J Mater Sci (2010) 45:2995–3000
DOI 10.1007/s10853-010-4300-3

Electrodeposition of $CuInSe_2$ in citrate-containing electrolytes

M. A. Frontini · M. Vázquez

Received: 4 November 2009 / Accepted: 3 February 2010 / Published online: 17 February 2010

Abstract $CuInSe_2$ is a frequent constituent of solar cells. Low-cost solar cells can be prepared by electrodeposition from a single bath, provided that the multiple variables affecting the process can be properly tuned. Our design includes an n-layer of TiO_2 (dense and/or nanoporous), on top of which a p-layer of $CuInSe_2$ is electrodeposited. The TiO_2 layer is supported on conductive glass. When $CuInSe_2$ is applied onto TiO_2, a p–n junction is formed by which sunlight could be transformed into electricity. $CuInSe_2$ films have been prepared by electrodeposition from a single bath aqueous solution. Citrate has been used as complexing agent, so as to shift the copper deposition potential in the negative direction, bringing it closer to the In deposition potential. Films are obtained potentiostatically at −0.8 V (vs. standard calomel electrode) for 1 h. The electrolyte consisted of 0.4 mol/L sodium citrate containing 3 mmol/L $CuCl_2$, 6 mmol/L $InCl_3$, and 5 mmol/L SeO_2. Different pH values between 4 and 6 are investigated. The samples are annealed in a furnace under flowing Ar at 350 °C for 15 min, which proves to be essential to improve the crystallinity of the $CuInSe_2$ films. TiO_2 and $CuInSe_2$ have been characterized using scanning electron microscopy, X-ray diffraction, and optical absorption spectroscopy. The morphology and the physical and optical properties are in good agreement with those reported in the literature. In order to investigate the photoresponse of the cells, current–voltage curves of prototype devices are performed in the dark and under light.

M. A. Frontini · M. Vázquez (✉)
División Corrosión, INTEMA, Facultad de Ingeniería,
Universidad Nacional de Mar del Plata, J. B. Justo 4302
B7608FDQ, Mar del Plata, Argentina
e-mail: mvazquez@fi.mdp.edu.ar

Introduction

$CuInSe_2$ (CISe) is a semiconductor with chalcopyrite structure that has exceptional photovoltaic application perspectives [1, 2]. Laboratory-scale solar cells made using this compound reached efficiency values of up to 13% [3]. One of the most significant advantages of CISe is the high radiation stability. It is also interesting to note the possibility of obtaining materials of both conductivity types, growing the sample under excess of Se (p-type), and deficit of Se or excess In (n-type) [4].

Among the various methods for depositing $CuInSe_2$, electrochemical deposition from aqueous solutions has been recognized for many decades as a technique of particular interest because it is cost-effective, technologically simple, and allows working over large surface areas [5]. Several attempts have been made to employ the one-step process where the CISe film is potentiostatically grown by co-deposition of Cu, In, and Se simultaneously [6–9]. An important problem that has been found when using this approach is with regard to controlling the composition of the resulting deposit. It has been shown that the film composition should be very close to that of CISe to obtain high efficiencies in thin film solar cell. This stoichiometric relation between the Cu, In, and Se atoms is directly related to the experimental conditions (temperature, substrate, and potential) and to the concentration of the various ions in the electrolyte. The fact that the reduction potentials of Cu, In, and Se are too far apart can be a problem when attempting one-step electrodeposition. This problem has been overcome by using complexing agents (such as citric acid, triethanolamine, cyanide ions, etc.) to reduce the activity of copper ions and thus, to shift the copper deposition potential in the negative direction, and bring it closer to the In deposition potential [10–13]. Pottier and Maurin [14] used a

complexing citrate solution during CISe electrodeposition and suggested that rather than shifting the equilibrium potential, the main function of the complexing agent is to promote the formation of a more crystalline compound. In the presence of citrate, charge transfer reactions occur in several steps, lowering the deposition rate and improving the overall quality of the film. The use of citrate is also convenient taking into account that it is neither toxic nor hazardous and that it contributes in buffering the solution pH. Finally, citrate ions in the electrolyte make the electrodeposition of CISe possible at pH values that are much less acidic than those used in previous investigations of similar systems [15, 16]. This can be important when CISe has to be prepared on top of semiconductor oxide layers that dissolve in more acidic electrolytes, such as ZnO. Thus, the procedure can be useful in the fabrication of superstrate-type CISe thin film solar cells.

In this study, we investigate the effects of using a slightly acidic electrolytic bath on the composition, morphology, and electronic properties of $CuInSe_2$ prepared by electrodeposition on dense and nanostructured TiO_2.

Experimental

$CuInSe_2$ (CISe) films are produced by electrodeposition from an electrolytic bath containing citrate as complexing agent. Electrodeposition is carried out at constant potential onto two different substrates, prepared as described elsewhere [15]:

(i) conductive tin-coated glass covered with dense TiO_2 (TCO/d-TiO_2) prepared by spray pyrolysis. The approximate thickness of the TiO_2 layer is 150 nm.
(ii) conductive tin-coated glass covered with a double layer of dense and nanoporous TiO_2 (TCO/d-TiO_2/nano-TiO_2) prepared by doctor blade. The approximate thickness of the TiO_2 layer is 1 μm.

The citrate medium is a 0.4 mol/L sodium citrate solution, containing 3 mmol/L $CuCl_2$, 6 mmol/L $InCl_3$, and 5 mmol/L SeO_2. The pH of the solution is adjusted with diluted solutions of HCl and NaOH to be between 4 and 6. Prior to the electrodeposition, the solution is purged with nitrogen (N_2), while the bath temperature is maintained at room temperature.

The films are obtained at −0.8 V (vs. standard calomel electrode (SCE)) for 1 h, using a three-electrode configuration. An SCE is used as reference, and a Pt (wire) is used as the counter electrode. Cyclic voltammograms are obtained using the same cell and are recorded at scan rate of 10 mV s^{-1} (in the positive direction first). Current and potential are controlled using a Solartron Instrument model 1280B.

In order to improve the crystallinity, the CISe films are annealed in flowing Ar at 350 °C for 15 min.

The thickness (T) of the samples is determined by measuring the total electrical charge circulating through the electrical cell during deposition, using Eq. 1, based on Faraday's law,

$$T = \frac{1}{n\,F\,A}\left(\frac{i\,t\,M}{\rho}\right) \tag{1}$$

where n is the number of electrons transferred, F Faraday's number, A the electrode area ($A = 1.26$ cm^2), i the current, t the deposition time, M the formula weight, and ρ the density. The formula weight and density used are $M = 336.28$ g mol^{-1} and $\rho = 5.77$ g cm^{-3} [17]. This is an approximation, since the formula weight and density vary with the film composition, and the efficiency of the electrodeposition process is assumed to be 100%. The number of electrons transferred is $n = 13$ according to the total electrode reaction:

$$Cu^{+2} + In^{+3} + 2\ SeO_2 + 8\ H^+ + 13\ e^- \rightarrow CuInSe_2 + 4\ H_2O. \tag{I}$$

The crystalline structure is determined from X-ray diffraction (Bruker D8 Advanced Diffractometer) using Cu K_α radiation and Ni–Cu slits filter. The diffraction patterns are recorded from $2\theta = 10°$–$80°$. The operation voltage and current used are 40 kV and 40 mA, respectively. The crystallite size is calculated by Scherrer's equation (Eq. 2):

$$L = \frac{K\lambda}{\beta_m \cos\theta}, \tag{2}$$

where L is the average crystallite size, β_m the full width of the peak at half of the maximum intensity (rad), λ the wavelength of X-ray radiation (1.5406 Å), and K a constant related to the crystallite shape and normally is taken as 0.9. The instrumental broadening contribution (β_{inst}) is determined using a Si reference at $2\theta = 33.11°$. Its contribution is found to be $\beta_{inst} = 3.133 \cdot 10^{-3}$ rad.

The morphology of the films is examined by scanning electron microscopy (SEM), using a JEOL JSM-6460LV microscope. The composition of the passive layer is analyzed by energy dispersive X-ray spectroscopy (EDX) investigations. The system used is an EDAX Genesis XM4—Sys 60, equipped with Sapphire Si(Li) detector and Super Ultra Thin Window of Be.

The optical properties of the films, such as absorption coefficient and the direct band gap energy E_g, are calculated from the transmission spectra recorded between 200 and 1,100 nm. These measurements are carried out using a commercial double-beam spectrophotometer Shimadzu UV160.

In order to investigate the photoresponse of the cells, current–voltage curves of devices such as SnO_2:F/

TiO_2(100 nm)/CISe/graphite and SnO_2:F/TiO_2(100 nm)/nc-TiO_2/CISe/graphite are performed in the dark and under Xe-lamp illumination. The graphite electrodes are coated onto the samples with conductive graphite ink. Electrode area (0.031 cm^2) is defined using a mask. In all the electrical measurements, the graphite electrode is the working electrode, while the TCO film serves as the counter/reference electrode. Thus, in forward bias, the graphite film is positive relative to the TCO electrode. The light source is a 150-W Xe-lamp coupled with a 380-nm UV filter. The light intensity is determined using a Si-photodiode.

Results and discussion

Citrate ions (Cit) are frequently used as ligands to form transition metal ions complexes with applications in biology, chemistry, and technology. The chemistry involving the citrate–copper complexation is far from simple, as citrate ions derive from an organic acid with three carboxylic groups and a ternary hydroxyl group. More than 14 copper-citrate chelates have been mentioned in the literature, such as $CuCit^-$, CuCitH, $CuCit_2H_2$, Cu_2Cit^+, etc. [18].

If the electrolyte is very acidic ($0 < pH < 3$), then citrate ions are protonated, and their ability to form complexes decays. Voltammetric studies performed at pH = 2 showed no effect in shifting the deposition potential of CISe, most likely due to the above reason [8]. At pH 4 and higher, Cu^{2+} ions and citrate ions form stronger complexes. In the present experimental conditions, CuCitH is the dominant species, as discussed by Daniele et al. [19], where the formation constant can be written as:

$$Cu^{2+} + Cit^{3-} + H^+ \leftrightarrows CuCitH$$
$$\beta = [CuCitH]/\left(\left[Cu^{2+}\right]\left[Cit^{3-}\right]\left[H^+\right]\right).$$

For this reaction, it has been reported that $\log \beta = 9.55$. An excess of Cit guarantees that the concentration of Cu^{2+} is notoriously reduced. This, in turn, shifts the copper ions reduction potential toward more negative values, bringing it closer to the deposition potential of indium(III) ions.

In this study, the electrochemical behavior of the Cu–In–Se system is studied by cyclic voltammetry on different substrates. In every case, the substrate is another semiconductor, supported in turn on conductive glass. The presence of a semiconductor increases the resistivity of the substrate, and, for this reason, the recorded current densities are low. Figure 1 shows the voltammetric responses on TCO/d-TiO_2 at pH 4 and 6. In both solutions, two cathodic peaks are observed. The behavior of the system is similar in both conditions. Only a slight difference in the position of the cathodic peak is observed (−0.91 V at pH 6 and −1.10 V at pH 4). This difference is in good agreement with that expected in response to the pH variation, according to reaction (I). Figure 2 shows the voltammetric response on TCO/d-TiO_2/nc-TiO_2 at pH 4 and 6. Again, the difference in the behavior of the two systems appears as expected. At pH 4, a cathodic peak is observed (−1.29 V) while only a shoulder is evident at pH 6 (−0.925 V). When compared to the current densities in Fig. 1, it can be seen that they are higher in the duplex substrate, even when the TiO_2 film is thicker, and presumably more resistive. The higher current densities are likely due to the fact that the scale is represented in terms of geometrical area, but here the real area of the nanoporous substrate is surely higher.

On the basis of the results presented in Figs. 1 and 2, −0.8 V is chosen as a suitable potential to produce the

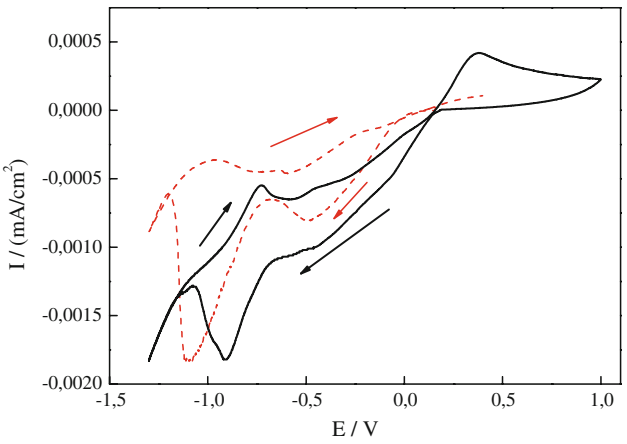

Fig. 1 Voltammograms of TCO/d-TiO_2 at pH 4 (*dash line*) and 6 (*full line*) in 0.4 mol/L sodium citrate containing 3 mmol/L $CuCl_2$, 6 mmol/L $InCl_3$, and 5 mmol/L SeO_2. Scan rate is 10 mV s^{-1}. The *arrows* indicated the direction of the potential scan

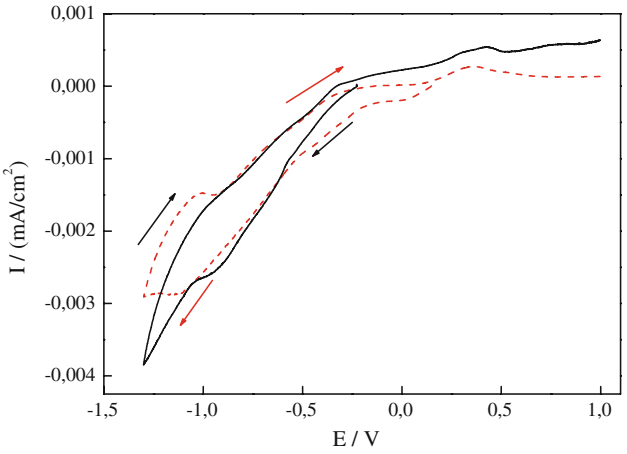

Fig. 2 Voltammograms of TCO/d-TiO_2/nc-TiO_2 at pH 4 (*dash line*) and 6 (*full line*) in 0.4 mol/L sodium citrate containing 3 mmol/L $CuCl_2$, 6 mmol/L $InCl_3$, and 5 mmol/L SeO_2. Scan rate is 10 mV s^{-1}. The *arrows* indicate the direction of the potential scan

Table 1 Thickness of $CuInSe_2$ electrodeposited in the various conditions tested

	Thickness (μm)	
	TCO/d-TiO_2	TCO/d-TiO_2/nc-TiO_2
pH 4	0.922	1.253
pH 6	1.184	1.908

electrodeposited CISe films. Table 1 shows the thickness of the deposits calculated using Eq. 1 at both pH values. It can be seen that the deposit on TCO/d-TiO_2/nc-TiO_2 is thicker than the one on the other substrate.

The annealed films are characterized by XRD on the different substrates at both pH values (Figs. 3, 4). Annealing significantly improves the crystallinity of the

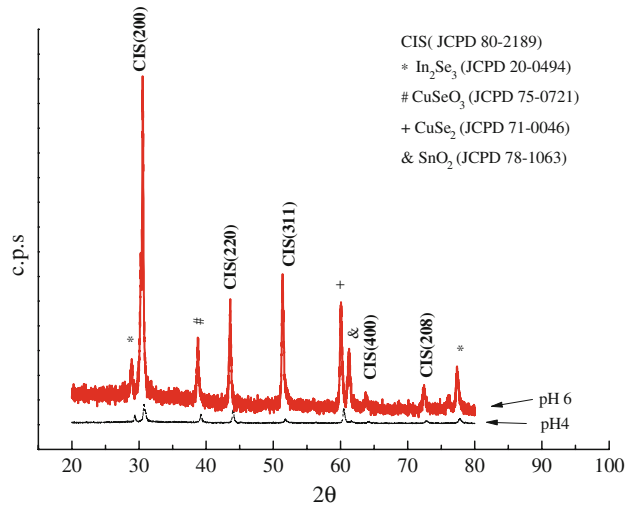

Fig. 3 X-ray diffraction diagrams of the $CuInSe_2$ electrodeposited on TCO/d-TiO_2 at pH 4 and 6

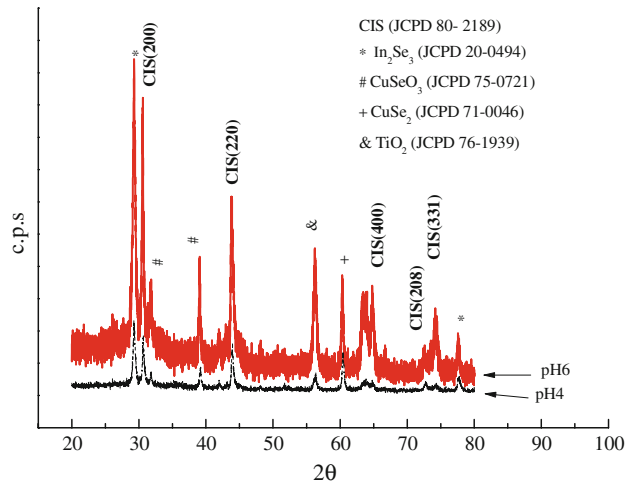

Fig. 4 X-ray diffraction diagrams of the $CuInSe_2$ electrodeposited on TCO/d-TiO_2/nc-TiO_2 at pH 4 and 6

CISe films, as discussed in a previous study [15]. A series of CISe characteristic peaks are identified, such as (200), (220), (400), (208), and (311). These peaks correspond to the chalcopyrite phase of the $CuInSe_2$. Other diffraction peaks are observed, attributed to TiO_2, SnO_2, In_2Se_3, $CuSe_2$, and $CuSeO_3$. $CuSe_2$ formation has been reported before by other authors [11, 20]. The results of crystallite size (L) are presented in Table 2. According to the Scherrer equation, the crystallite size is similar for two substrates.

Absorption spectra are recorded for annealed samples at different pH values. These data can be represented by $(\alpha h\nu)^2$ versus ($h\nu$) plots, so as to determine the band gap values (E_g) of the films (Figs. 5, 6). E_g values are determined by extrapolation from the photon energy axis and range from 1.04 to 1.48 eV, which are very similar to CISe films produced using different techniques or electrodeposited using a metal as substrate [21–25].

The analysis of the surface morphology and composition of the films is carried out by SEM and EDX. Figure 7a shows a uniform deposit with a compact surface and a multi-nuclei cauliflower shape. Figure 7b exhibits particles of bigger size with a more remarkable cauliflower appearance. The difference in structure is in agreement with the different thicknesses reported in Table 1. Average percentages reflect the proportion of each element present in each sample, which when compared to the stoichiometric composition also reveals the presence of secondary phases.

Table 2 Variation of crystallite size on two substrates at pH values 4 and 6

	Crystallite size (nm)			
	$D_{(200)}$		$D_{(220)}$	
	pH 4	pH 6	pH 4	pH 6
TCO/d-TiO_2	19	23	25	27
TCO/d-TiO_2/nc-TiO_2	26	27	23	20

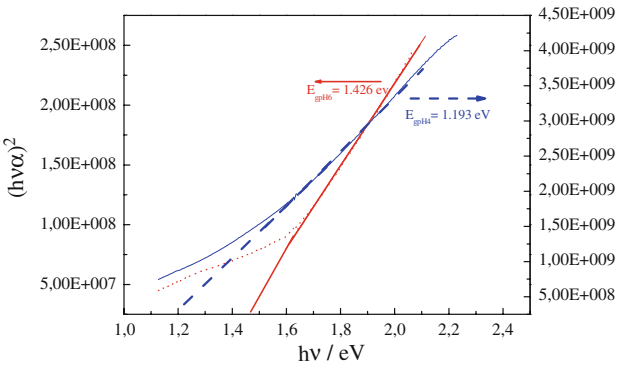

Fig. 5 Graphic representation of $(\alpha h\nu)^2$ versus $h\nu$ for $CuInSe_2$ electrodeposited on TCO/d-TiO_2 for E_g determination at pH 4 (*dot line*) and 6 (*full line*)

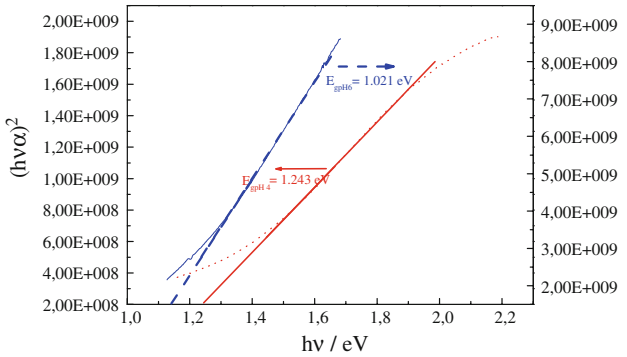

Fig. 6 Graphic representation of $(\alpha h\nu)^2$ versus $h\nu$ for $CuInSe_2$ electrodeposited on TCO/d-TiO_2/nc-TiO_2 for E_g determination at pH 4 (*dot line*) and 6 (*full line*)

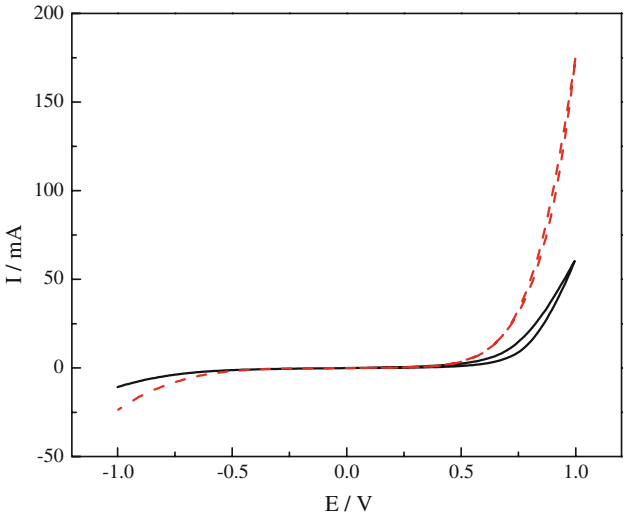

Fig. 8 *I–V* curves of a CISe film electrodeposited on TCO/d-TiO_2/nc-TiO_2 electrode at pH = 6. *Solid line* recorded without illumination, and *broken line* recorded under illumination

Finally, the photoelectrochemical response of CISe films is analyzed. The set-up consists of SnO_2:F/TiO_2(100 nm)/d-TiO_2/nc-TiO_2/CISe/graphite. The CISe is electrodeposited at −0.8 V for 1 h at pH = 6. As can be seen in Fig. 8, the dark response shows diode behavior with a good rectification. A considerable increment in the current can also be seen when the sample is illuminated, for potential values higher than 0.5 V. Under irradiation, the presence of the nanostructured TiO_2 improves the performance of the cell, probably due to the bigger contact surface between the n- and p-semiconductors. Smaller differences are found in the current increment for CISe deposited on different substrates. The low current density values in the vicinity of V_{oc} can be related to the resistance and thickness of the TiO_2/nc-TiO_2 (bi)layer. The low energy conversion in the illuminated *I–V* curve can also be associated to fast electron–hole recombination in the TiO_2/CISe interface. Even

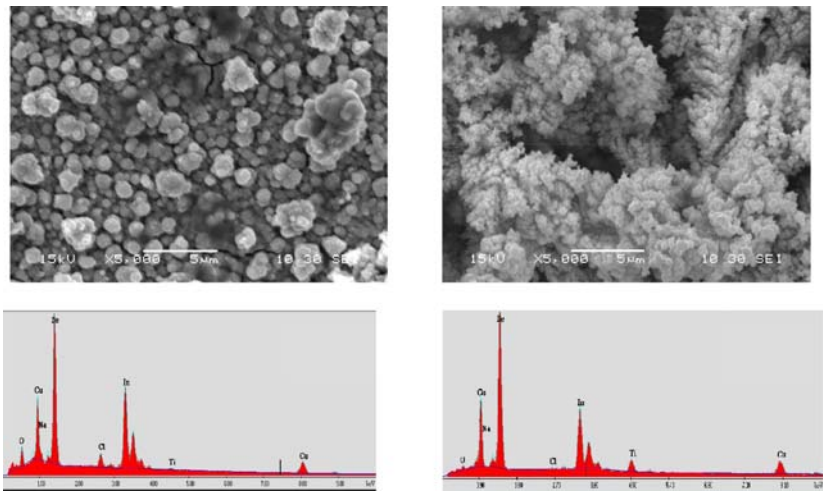

% Se (46.9) *	37.32	42.29
%Cu (18.8) *	16.74	21.98
% In (34.2) *	36.62	30.15

Fig. 7 SEM images of $CuInSe_2$ electrodeposited at pH 6: on TCO/d-TiO_2 (**a**), on TCO/d-TiO_2/nc-TiO_2 (**b**). Average compositions derived from EDX spectra are also indicated. * Stoichiometric compositional values

when the values of the open circuit potential (V_{oc}) and the short-circuit current density (J_{sc}) are minimal, the presence of a photocurrent proves the benefit of electrodepositing CISe using slightly acidic electrolytes on top of a nanocrystalline substrate. Through optimization of the etching processes and introduction of a buffer layer together with rapid thermal annealing, the conversion efficiency is expected to improve significantly.

Conclusions

Thin films of $CuInSe_2$ are prepared by one-step electrodeposition method using slightly acidic and near neutral electrolytes containing citrate ions as complexing agent. The electrodeposition of chalcopyrite from a single bath and using another semiconductor as substrate proved to be successful. The results are promising in the field of photovoltaic solar cells because they show that CISe can be electrodeposited on top of n-type semiconductors at pH values that guarantee the stability of other prospective candidates, such as ZnO.

$CuInSe_2$ has been characterized using different physical methods. The results indicate that the material is crystalline and has a chalcopyrite structure. The thickness is higher when the pH is 6. The optical band gap yielded values lying between 1.02 and 1.45 eV, which are appropriate for photovoltaic applications.

The current–potential curves in the dark show a very good diode behavior. Even when some photoconductivity is clearly present, photovoltaic energy conversion is still very small. This could be partially due to the electronic properties of TiO_2, as well as to the presence of secondary phases such as $CuSe_2$. Ongoing studies aim at incorporating an electrochemical-etching stage, which could be used an alternative to those based on cyanide.

Acknowledgements The authors acknowledge the financial support received from the National Research Council of Argentina (CONICET), the Agencia Nacional de Promoción Científica y Tecnológica (PICT 22-21440/04 and 1144/07), and the Universidad Nacional de Mar del Plata.

References

1. Kemell M, Ritala M, Leskelä M (2005) Crit Rev Solid State Mater Sci 30:1
2. Zunger A (2007) Thin Solid Films 515:6160
3. Kushiya K (2009) Sol Energy Mater Sol Cells 93:1037
4. Gorley PM, Khomyak VV, Vorobiev YV, González-Hernández J, Horley PP, Galochkina OO (2008) Sol Energy 82:100
5. Qiu CX, Shih I (1987) Sol Energy Mater Sol Cells 15:219
6. Gujar T, Shinde V, Park J, Lee H, Jung K, Joo O (2009) J Electrochem Soc 156:E8
7. Jost S, Hergert F, Hock R, Schulze J, Kirbs A, Vob T, Purwins M (2007) Sol Energy Mater Sol Cells 91:1669
8. Kemell M, Ritala M, Saloniemi H, Leskela M, Sajavaara T, Rauhala E (2000) J Electrochem Soc 147:1080
9. Sene C, Calixto ME, Dobson K, Birkmire R (2008) Thin Solid Films 516:2188
10. Thouin L, Vedel J (1995) J Electrochem Soc 142:2996
11. Molin AN, Dikusar AI, Kiosse GA, Petrenko PA, Sokolovsky AI, Saltanovsky YG (1994) Thin Solid Films 237:66
12. Bhattacharya NR, Rajeshwar K (1986) Sol Cells 16:237
13. Beyhan S, Suzer S, Kadirgan F (2007) Sol Energy Mater Sol Cells 91:1922
14. Pottier D, Maurin G (1989) J Appl Electrochem 19:361
15. Valdes M, Frontini MA, Vazquez M, Goossens A (2007) Appl Surf Sci 254:303
16. Valdes M, Vázquez M, Goossens A (2008) Electrochim Acta 54:524
17. Weast RC (1987) Handbook of chemistry and physics, 67th ed. CRC Press, Inc, Boca Raton, FL
18. Rode S, Christophe H, Vallieres C, Matlosz M (2004) J Electrochem Soc 151:C405
19. Daniele PG, Ostacoli G, Zerbinati O, Sammartano S, De Robertis A (1988) Trans Met Chem 13:87
20. Thouin L, Rouquette-Sanchez S, Vedel J (1993) Electrochim Acta 38:2387
21. Gobeaut A, Laffont L, Tarascon JM, Parissi L, Kerrec O (2009) Thin Solid Films 517:4436
22. Kang F, Ao JP, Sun GZ, Sun Y (2009) Mater Chem Phys 115:516
23. Akl AA, Afify HH (2008) Mater Res Bull 43:1539
24. Mehdaoui S, Benslim N, Aissaoui O, Benabdeslem M, Bechiri L, Otmani A, Portier X, Nouet G (2009) Mater Charact 60:451
25. Shah NM, Ray JR, Kheraj VA, Desai MS, Panchal CJ, Rehani B (2009) J Mater Sci 44:316. doi:10.1007/s10853-008-3046-7